

# UC Irvine

## UC Irvine Previously Published Works

### Title

Two-phase structural refinement of La<sub>2</sub>CuO<sub>4.032</sub> at 15 K

### Permalink

<https://escholarship.org/uc/item/5d35v5xk>

### Journal

Physica C Superconductivity, 170(1-2)

### ISSN

0921-4534

### Authors

Chaillout, C  
Chenavas, J  
Cheong, SW  
[et al.](#)

### Publication Date

1990-09-01

### DOI

10.1016/0921-4534(90)90233-5

### Copyright Information

This work is made available under the terms of a Creative Commons Attribution License, available at <https://creativecommons.org/licenses/by/4.0/>

Peer reviewed

## Two-phase structural refinement of $\text{La}_2\text{CuO}_{4.032}$ at 15 K

C. Chaillout<sup>a</sup>, J. Chenavas<sup>a</sup>, S.W. Cheong<sup>b</sup>, Z. Fisk<sup>c</sup>, M. Marezio<sup>a,b</sup>, B. Morosin<sup>d</sup>  
and J.E. Schirber<sup>d</sup>

<sup>a</sup> *Laboratoire de Cristallographie, CNRS-UJF, 166X, 38042 Grenoble cedex, France*

<sup>b</sup> *AT&T Bell Laboratories, Murray Hill, NJ 07974, USA*

<sup>c</sup> *Los Alamos National Laboratory, NM 87545, USA*

<sup>d</sup> *Sandia National Laboratories, Albuquerque, NM 87185, USA*

Received 24 April 1990

Revised manuscript received 14 June 1990

A two-phase refinement of a crystal for the compound  $\text{La}_2\text{CuO}_{4+\delta}$  ( $\delta=0.032$ ), based on the neutron diffraction data collected at 15 K with the D9 diffractometer at ILL, using  $\lambda=0.48 \text{ \AA}$ , has been carried out. One phase (30%) consists of stoichiometric  $\text{La}_2\text{CuO}_4$  domains, while the other (70%) of oxygen-rich  $\text{La}_2\text{CuO}_{4.048}$  domains. The percentages of each phase, which have been refined together with the other parameters (scale factor, positional parameters, thermal factors and occupancy factors of the oxygen atoms), agree very well with the value determined from  $\chi_{AC}$  measurements. The  $\text{La}_2\text{CuO}_{4.048}$  structure is essentially the same as the average structure reported in ref. [1], the only difference being the oxygen content which is found to be  $\delta' = \delta/0.70$ . The extra oxygen, O(4), is found to be in between two LaO layers in a similar position as the oxygen atoms located between two Nd layers in the  $\text{Nd}_2\text{CuO}_4$  structure. The insertion of extra oxygen causes the displacement of some of the oxygen O(1) towards the O(3) positions. Different models are proposed for the distortion induced by this insertion according to the experimental value, 3.3 [6], found for the ratio of the amount of O(3) to that of O(4). If this ratio is assumed to be 3 and the O(3) atoms are localized about the insertion, then the formation of a short O(4)–O(3) bond would occur. The models not requiring the formation of the short bond correspond to ratios of 2 or 4. In the latter case there would be four displaced O(1), but due to the rigidity of the oxygen octahedra only two O(3) would be bonded to O(4), the other two being the apically opposite oxygen atoms of the same octahedra.

In 1989 Chaillout et al. reported the crystal structure determination of superconducting  $\text{La}_2\text{CuO}_{4+\delta}$ . Single-crystal neutron diffraction data were taken at room temperature and at 15 K by using the D9 diffractometer at ILL. The details of the data collection together with those of the structural refinement are given in ref. [1]. A short wavelength (0.48 Å) was chosen in order to solve the twinning problem present in the crystal used. We found that the La/Cu ratio was 2 within our precision (0.5%) and that the oxygen stoichiometry was 4.032.

The unit cell ( $5.350 \times 13.148 \times 5.398 \text{ \AA}$ ) of the  $\text{La}_2\text{CuO}_4$  structure comprises the sequence  $(\text{CuO}_2)_o - (\text{LaO})_c (\text{LaO})_o (\text{CuO}_2)_c (\text{LaO})_o (\text{LaO})_c (\text{CuO}_2)_o$ . The oxygen atoms of the (LaO(1)) layers are the apices of the  $\text{CuO}(2)_6$  octahedra. A schematic representation of the structure of the superconducting, oxygen-doped material is given in fig. 1. The excess

oxygen (O(4)) is localized between two successive LaO layers, in the special position  $(\frac{1}{4}y\frac{1}{4})$  with  $y=0.243$ . We also found that the insertion of the O(4) induces a local distortion of part of the apical oxygen (O(1)) sublattice. The structural refinement was carried out using  $\text{Cmca}$  as the space group; the O(1) sites were not found to be fully occupied and sites, called O(3), located at about 0.75 Å from O(1) were found to be partially occupied in such a way that  $p(\text{O}(1)) + p(\text{O}(3)) = 1$ , where  $p(\text{O})$ 's are the occupancy factors for these two oxygen sites. From the value of  $p(\text{O}(3))$  and  $p(\text{O}(4))$  it seems that O(4) is responsible for the displacement of three apical oxygen O(1) towards the O(3) positions. In this case there necessarily exists a short O–O distance, which, from the magnitude of the difference from a normal O–O distance, could be indicative of a peroxide bond.

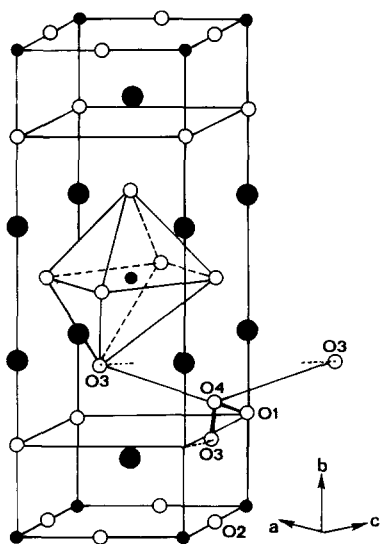


Fig. 1. A schematic representation of the structure of  $\text{La}_2\text{CuO}_{4.032}$ . Only one half orthorhombic cell is shown. The plane defined by the diagonal of the  $\text{CuO}$  plane ( $c$ -axis) and vertical ( $b$ -axis) contains the La and O(1) atoms slightly shifted from the edges of the box shown (which represents the tetragonal basis at higher temperatures).

Jorgensen et al. [2] showed by powder neutron diffraction that in a polycrystalline sample of superconducting  $\text{La}_2\text{CuO}_{4+\delta}$  with  $\delta \approx 0.03$ , a phase separation occurred at about 320 K. The powder pattern below this temperature was interpreted as the co-existence of two phases in the ratio 70:30, one non-superconducting, having essentially  $\text{La}_2\text{CuO}_4$  stoichiometry, and one oxygen-rich superconducting having  $\text{La}_2\text{CuO}_{4+\delta}$  stoichiometry. Their powder neutron diffraction experiments yielded accurate results for the lattice parameters as a function of temperature, but no definite conclusion was reached for the space group of  $\text{La}_2\text{CuO}_{4+\delta}$ . The separation into two phases was recently confirmed by Zolliker et al. [3] by powder X-ray synchrotron radiation and neutron diffraction using a sample of superconducting  $\text{La}_2\text{CuO}_{4+\delta}$  with  $\delta \approx 0.03$ . Below 290 K, the  $\text{Cmca}$  phase was observed to evolve steadily down to about 250 K, at which point the two phases were present in roughly equal proportions. Both of these two groups of investigators measured the variation with temperature of the lattice parameters. They found that below the phase separation transition one of the

cell parameters of the two phases was essentially identical. The choice of space group  $\text{Cmca}$  and  $\text{Fmmm}$  for  $\text{La}_2\text{CuO}_4$  and  $\text{La}_2\text{CuO}_{4+\delta}$ , respectively, was based on the systematic absence from the  $\text{La}_2\text{CuO}_{4+\delta}$  pattern of those reflections which are allowed for  $\text{Cmca}$  and violate the F-centering. Jorgensen et al. [4] justified their choice of space group, by pointing out that the similar compound  $\text{La}_2\text{NiO}_{4+\delta}$  belongs to the  $\text{Fmmm}$  space group.

Discussions with various members of both groups stimulated us to carry out additional and continuing studies on the same crystal used in ref. [1]. Several ( $hkl$ ) reflections were scanned as a function of temperature. These measurements were done both by X-ray diffraction using a conventional source ( $\lambda[\text{Cu K}\alpha] = 1.5418 \text{ \AA}$  and  $\lambda[\text{WLa}\alpha] = 1.4800 \text{ \AA}$ ) and by neutron diffraction using the D10 diffractometer at ILL with a considerably longer wavelength ( $1.26 \text{ \AA}$ ) than that used for the data collection ( $0.48 \text{ \AA}$ ) with D9 [5]. By X-ray diffraction we scanned the following reflections: (0 14 0), (1 15 1), (2 14 2), (3 11 3), (1 11 3), (3 11 1) and (5 3 3) between 295 K and 118 K. The low temperatures were attained by the use of a cold gas blower. The phase separation was observed for the scans carried out at 273 K and below this temperature. For all of these reflections the contribution of the oxygen-poor  $\text{La}_2\text{CuO}_4$  phase to the total intensity increased from the phase separation temperature until 230 K, after which it remained constant (see fig. 2).

The total oxygen contribution to the scattering for the reflections mentioned above is much smaller than that from the cations. For this type of reflections, the phase identified as  $\text{La}_2\text{CuO}_{4+\delta}$  by Jorgensen et al. has the strongest intensity. On the other hand, these reflections are allowed by both space groups, either  $\text{Cmca}$  or  $\text{Fmmm}$  and are also affected by the twinning. Therefore, they do not reveal whether or not the  $\text{La}_2\text{CuO}_{4+\delta}$  structure is F-centered. The assignment of the space group is important towards defining models necessary for the formation of a short O-O bond in  $\text{Cmca}$  whereas such necessity does not exist for  $\text{Fmmm}$  (see fig. 3).

The untwinned ( $hkl$ ) reflections with either  $h=2n$ ,  $k=2n$  and  $l=2n+1$  or with  $h=2n+1$ ,  $k=2n+1$  and  $l=2n$ , are not easily detectable by X-ray diffraction because they are due mostly to the oxygen atoms. This is why we switched to neutron diffraction. It was ob-

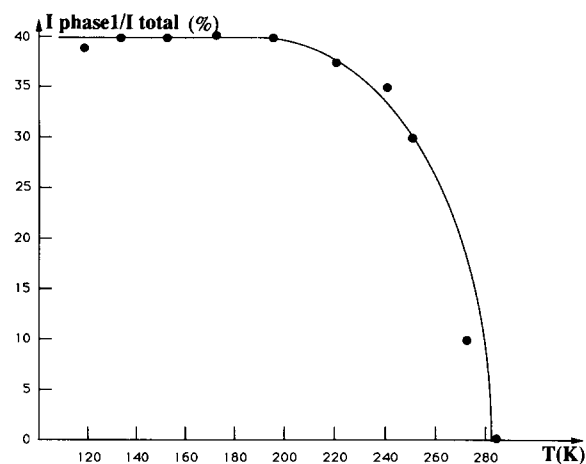


Fig. 2. Variation of the contribution of phase 1 oxygen-poor ( $\text{La}_2\text{CuO}_4$ ) to the total intensity of the (0 140) reflection as a function of temperature.

served that these reflections underwent well-defined splittings at the phase separation. Since they are not allowed by the F-centering, the observance of this splitting strongly indicates that  $\text{La}_2\text{CuO}_{4+\delta}$  does not belong to the Fmmm space group. It must be pointed out that for these reflections the intensity due to the  $\text{La}_2\text{CuO}_4$  phase is much stronger than that due to the  $\text{La}_2\text{CuO}_{4+\delta}$  phase (see fig. 4) because of the structural details discussed above.

Since the phase separation occurred in our crystal as well and the short wavelength resulted in unresolved peaks, the structure previously determined and reported in ref. [1] is an average structure. In order to determine more precisely the position of O(4), its occupancy factor which corresponds to the excess oxygen  $\delta$ , and the distances between O(4) and the other oxygen atoms, we have carried out a simultaneous refinement of the structures of both phases,  $\text{La}_2\text{CuO}_4$  and  $\text{La}_2\text{CuO}_{4+\delta}$ , based on the neutron diffraction data collected with D9 at 15 K, which consisted of 1073 different  $hkl$  peaks. This has been done by the use of the MXD refinement program [6].

Because of the observed splitting of the  $hkl$ 's which violate F-centering, we assigned the Cmca space group to both structures (table I); hereafter, an added digit to each atom defines the phase. The phase separation occurs at a lower temperature than that of the tetragonal to orthorhombic transition, therefore,

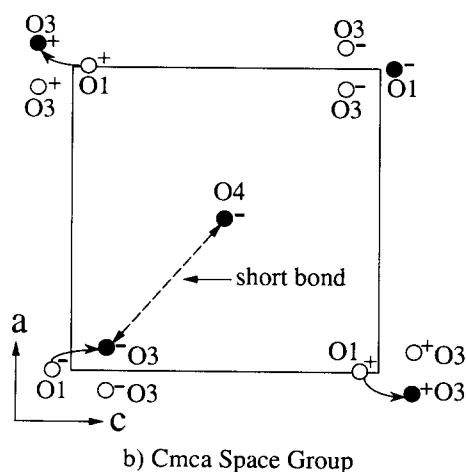
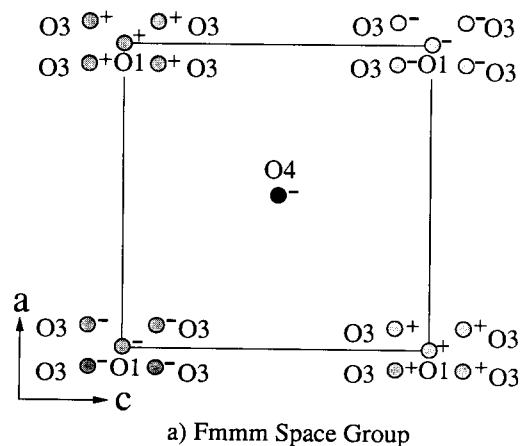


Fig. 3. A projection of the section containing O(12), O(32) and O(42) atoms on the  $ac$ -plane (only  $a/2$  by  $c/2$  shown; - and + superscripts indicate atoms below or above the  $y=1/4$  plane, respectively) for the case of: (a) Fmmm space group, (b) Cmca space group. For every O(4) inserted, three O(1) move while one neighboring O(1) stays fixed. The one staying fixed is already furthest away (near  $\frac{1}{2}0\frac{1}{2}$ ) on right). Of the three that move, one forms the short bond while the other two move further away as indicated by arrows. Filled circles represent occupied oxygen positions. This model corresponds to  $R \text{O}(3)/\text{O}(4)=3$ .

both phases are twinned. The same twinning percentage was assumed for the  $\text{La}_2\text{CuO}_4$  and  $\text{La}_2\text{CuO}_{4+\delta}$  domains, (46%) which was obtained during the refinement of ref. [1]. The starting parameters were as follows: the fraction of phase 2 was taken as  $p_\phi=0.50$ ; hence, that for phase 1 becomes  $1-p_\phi=0.50$ ; the position parameters were those of

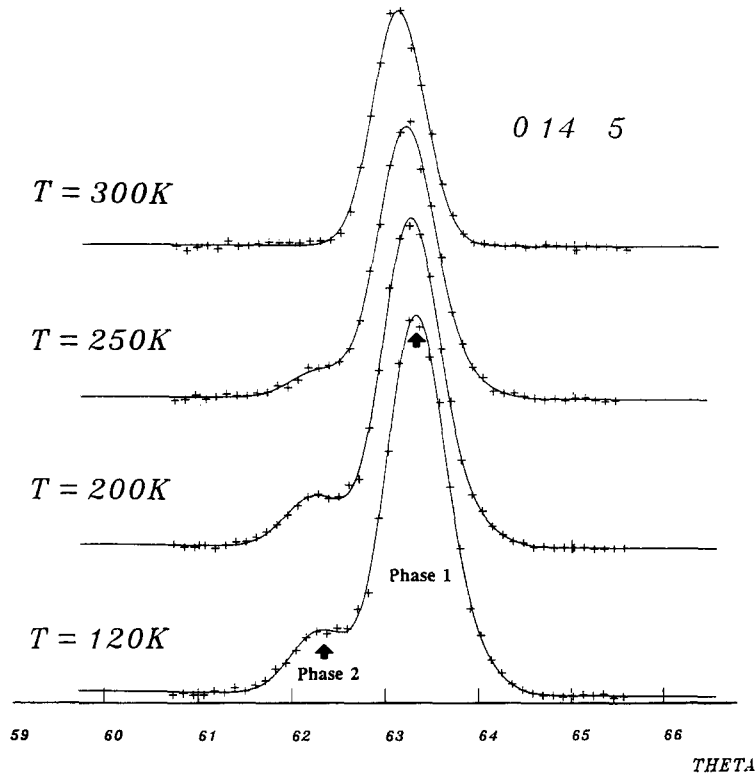


Fig. 4.  $\omega-2\theta$  scan of (0 1 4 5) reflection (neutron diffraction) between 300 K and 120 K showing the sudden phase separation. Crosses represent experimental points. The arrow indicates the peak's positions as determined from fitting with Gaussian functions.

Table I

Special positions occupied in  $\text{La}_2\text{CuO}_4$  and  $\text{La}_2\text{CuO}_{4+\delta}$  in space group  $\text{Cmca}$  (an additional index has been added to define atoms of each phase).

		Phase 1	Phase 2
La	8f(m)	0, $Y_{\text{La}(1)}$ , $Z_{\text{La}(1)}$	0, $Y_{\text{La}(2)}$ , $Z_{\text{La}(2)}$
Cu	4a(2/m)	0, 0, 0	0, 0, 0
O(1)	8f(m)	0, $Y_{\text{O}(11)}$ , $Z_{\text{O}(11)}$	0, $Y_{\text{O}(12)}$ , $Z_{\text{O}(12)}$
O(2)	8e(2)	$\frac{1}{4}$ , $Y_{\text{O}(21)}$ , $\frac{1}{4}$	$\frac{1}{4}$ , $Y_{\text{O}(22)}$ , $\frac{1}{4}$
O(3)	16g(1)		$X_{\text{O}(32)}$ , $Y_{\text{O}(32)}$ , $Z_{\text{O}(32)}$
O(4)	8e(2)		$\frac{1}{4}$ , $Y_{\text{O}(42)}$ , $\frac{1}{4}$

ref. [1] for both phases; the occupancy factors of the oxygen atoms O(11), O(21) for phase 1 ( $\text{La}_2\text{CuO}_4$ ) were taken as being equal to unity while the occupancy factors of the oxygen atoms O(12), O(22), O(32) and O(42) for phase 2 ( $\text{La}_2\text{CuO}_{4+\delta}$ ) were given the values obtained for the average structure described in ref. [1], namely  $p_{\text{O}(12)}=0.943$ ,

$p_{\text{O}(22)}=1$ ,  $p_{\text{O}(32)}=0.024$ , and  $p_{\text{O}(42)}=0.016$ . The temperature factors were first isotropic and transformed in later refinement cycles to anisotropic for all atoms except for O(32) and O(42). Because of the similarity of the two structures, the correlation coefficients between various parameters can be high. This necessitated a constrained, damped approach

to the least-squares procedure to ensure convergence. During the first cycles of refinement only the scale factor, the positional parameters of all atoms except those of O(32) and O(42), and  $p_\phi$  were refined. For the latter parameter a value of 0.71 was obtained. During the following cycles,  $p_\phi$  was fixed at this value and the remaining parameters were varied. This was done in a sequential fashion, first the thermal factors, then the occupancy factors of the oxygen atoms for phase 1 and 2. In the fast cycles of refinement the following parameters were varied simultaneously: the scale factor, the twinning percentage,  $p_\phi$ , the positional parameters, the anisotropic thermal factors (isotropic for O(32) and O(42)), and the occupancy factors of all oxygen atoms of both phases. The final values are reported in table II. The  $R$ -factors are:  $R_w=4.45\%$ ,  $R_{uw}=3.10\%$  and  $\chi^2=4.18$ . The corresponding values for the refinement taking into account only one phase were:  $R_w=5.13\%$ ,  $R_{uw}=3.80\%$  and  $\chi^2=4.20$ .

It should be pointed out that for phase 2 the atomic displacements for La(2), O(22), and O(12) from the positions required in the space group Fmmm ( $z_{\text{La}(2)}=0$ ,  $y_{\text{O}(22)}=0$  and  $z_{\text{O}(12)}=0$ ) and their standard deviations are significant. The ratios between the positional parameters and their respective standard deviation are 26, 15 and 52 for La, O(2) and O(1), respectively. Nevertheless, the displacements in phase 2 are much smaller than those found in phase 1 for the corresponding atoms. The matrix correlation elements greater than 0.10 for  $z_{\text{La}(2)}$ ,  $y_{\text{O}(22)}$  and  $z_{\text{O}(12)}$  parameters are given in table III. There is a somewhat large correlation only between  $z_{\text{O}(12)}$  and  $U_{11\text{O}(12)}$ , the corresponding correlation matrix element being 0.75. Nevertheless, it should be pointed out that  $z_{\text{O}(12)}$  is 52 times its standard deviation. The final value for  $p_\phi$  is 0.69(0.03) which is in good agreement with that estimated by AC susceptibility ( $\approx 0.70$ ).

The stoichiometry of phase 1 is indeed  $\text{La}_2\text{CuO}_4$  while that of phase 2 is  $\text{La}_2\text{CuO}_{4.048}$  with the amount of O(32) and O(12) equal to 1 (recalling the multiplicity factors in table I) and the ratio of the amounts of O(32) and O(42) = 3.3(6). Note that the excess oxygen  $\delta(0.032)$  found with the one-phase refinement is indeed 69% of that found (0.048) with the two-phase refinement.

The cation–oxygen and oxygen–oxygen intera-

Table II

Positional, thermal and occupancy parameters for  $\text{La}_2\text{CuO}_4$  and  $\text{La}_2\text{CuO}_{4+\delta}$  (standard deviations are given in parentheses as errors in the last significant digit).

	Phase 1	Phase 2
YLa	0.3616(2)	0.36088(6)
ZLa	0.0096(5)	0.0053(2)
YO(1)	0.1843(2)	0.1823(1)
ZO(1)	-0.048(1)	-0.0261(5)
YO(2)	-0.0112(5)	-0.0031(2)
XO(3)		0.033(5)
YO(3)		0.185(2)
ZO(3)		0.105(4)
YO(4)		0.242(4)
PO(1)	0.99(1)	0.922(8)
PO(2)	0.99(1)	0.999(5)
PO(3)		0.040(4)
PO(4)		0.024(4)
$U_{11}\text{La}$	-0.002(1)	0.011(1)
$U_{22}\text{La}$	0.0056(7)	0.0018(2)
$U_{33}\text{La}$	0.004(1)	0.0008(7)
$U_{23}\text{La}$	0.0004(4)	-0.0005(4)
$U_{11}\text{Cu}$	0.001(2)	0.005(2)
$U_{22}\text{Cu}$	0.0043(9)	0.0051(4)
$U_{33}\text{Cu}$	0.001(2)	-0.000(1)
$U_{23}\text{Cu}$	-0.0002(6)	-0.0003(6)
$U_{11}\text{O}(1)$	0.005(1)	0.015(2)
$U_{22}\text{O}(1)$	0.0018(8)	0.0051(4)
$U_{33}\text{O}(1)$	0.006(2)	0.0087(7)
$U_{23}\text{O}(1)$	-0.0003(8)	-0.0000(8)
$U_{11}\text{O}(2)$	0.001(1)	0.011(1)
$U_{22}\text{O}(2)$	0.003(1)	0.0127(5)
$U_{33}\text{O}(2)$	0.003(1)	-0.000(1)
$U_{13}\text{O}(2)$	0.0008(6)	0.0006(4)
$U\text{O}(3)$		0.005 fixed
$U\text{O}(4)$		0.005 fixed
$p_\phi$		0.69(3)
$1-p_\phi$	0.31(3)	
$R_w=4.45\%$	$R_{uw}=3.10\%$	$\chi^2=4.18$

tomies for the two phases are given in table IV. The O(1)–O(4) and O(3)–O(4) bond values listed are all those possible; the specific values depend on the model deduced from the occupancy factors discussed below. These models depend on using integral values for displaced atoms and if one localizes the displacement about the insertion or allows the  $\text{CuO}_6$  octahedron to tip (i.e., a rigid octahedron). Further, the parameters  $p(\text{O}(1))$  and  $p(\text{O}(3))$  were varied independently during the refinement. It must be pointed out that the standard deviation (0.6)

Table III  
Matrix correlation elements greater than 0.1 for  $z_{\text{La}(2)}$ ,  $z_{\text{O}(12)}$  and  $y_{\text{O}(22)}$  parameters.

$z_{\text{La}(2)}$	$z_{\text{O}(12)}$	0.17
	$y_{\text{O}(22)}$	0.13
	$U_{11}\text{La}(2)$	0.34
	$U_{33}\text{La}(2)$	0.29
	$U_{33}\text{O}(12)$	0.33
$z_{\text{O}(12)}$	$y_{\text{O}(22)}$	0.15
	$z_{\text{O}(32)}$	0.47
	$U_{11}\text{Cu}(2)$	0.11
	$U_{33}\text{Cu}(2)$	0.15
	$U_{11}\text{O}(12)$	0.75
	$U_{33}\text{O}(12)$	0.32
	$P\text{O}(12)$	0.38
	$P\text{O}(32)$	0.30
$y_{\text{O}(22)}$	$U_{22}\text{O}(22)$	0.40
	$U_{33}\text{O}(22)$	0.10

for the ratio of the amount of O(3)/O(4) (hereafter  $R\text{O}(3)/\text{O}(4)$ ) does not take into consideration that  $p(\text{O}(3))$  was determined twice during the refinement; once directly  $p(\text{O}(3))$ , (0.040), and once indirectly from  $[1-p(\text{O}(1))]/2$ , (0.039).

The model nearest to that determined by  $R\text{O}(32)/\text{O}(42)=3.3(6)$ , consists of the presence of one O(42) which displaces three near-neighbor O(12) towards the positions O(32), forcing one of the four O(4)–O distances to be 1.59(4) Å (as suggested in fig. 3(b)). This value is shorter than that found with the one-phase refinement (1.64 Å) and thus closer to the O–O distances with peroxide character (1.48 Å). If  $R\text{O}(3)/\text{O}(4)$  were 2, only two O(1) atoms would be displaced towards the O(3) positions. Two cases exist: if such displacements are localized, these two atoms would be those which would increase their distance from O(4) (see fig. 3(b)). Thus, the formation of the short O(3)–O(4) distance would not occur. On the other hand, one could equally select a short distance together with the apically opposite O(3) as the appropriate model. Within a few estimated standard deviations of  $R\text{O}(3)/\text{O}(4) \geq 4$ , models would employ rigid octahedra. For example, for  $R\text{O}(3)/\text{O}(4)=4$ , a model can be envisaged in which only two O(1) nearest neighbors of O(4) would be displaced towards the O(3) positions, the other two displaced O(1) being those apically opposite. This case would be in a way equivalent to that corresponding to  $R\text{O}(3)/\text{O}(4)=2$  as only two O(3)

Table IV  
Selected interatomic distances.

	Phase 1	Phase 2
Cu–O(1)	2.437(1)×2	2.401(1)×2
Cu–O(2)	1.9057(2)×4	1.9005(1)×4
Cu–O(3)		2.50(3)×2
La–O(1)	2.352(2)×1	2.354(2)×1
	2.463(3)×1	2.592(3)×1
	2.750(4)×2	2.7369(3)×2
	3.070(3)×1	2.924(3)×1
La–O(2)	2.559(2)×2	2.624(2)×2
	2.710(2)×2	2.651(2)×2
La–O(3)		2.38(3)×2
		2.25(2)×2
		2.64(3)×2
		2.97(3)×2
		3.30(2)×2
La–O(4)		2.35(3)×2
		2.44(3)×2
O(1)–O(2)	3.096(3)×2	3.032(3)×2
	3.091(3)×2	3.092(3)×2
O(2)–O(2)	2.675(2)×2	2.675(2)×2
	2.715(2)×2	2.700(2)×2
O(1)–O(4)		2.06(3)×2
		2.15(2)×2
O(2)–O(3)		2.77(3)×2
		2.94(3)×2
		3.34(3)×2
		3.48(3)×2
O(3)–O(4)		1.59(4)×2
		1.86(3)×2
		2.44(3)×2
		2.62(3)×2

would be nearest neighbor to O(4) and, therefore, the formation of the short bond would not occur. For  $R\text{O}(3)/\text{O}(4)=6$  it would be like the case given above for  $R\text{O}(3)/\text{O}(4)=3$ , but employing rigid octahedra. More complex models involving close or adjacent O(4) defects are also possible. For example, a rigid octahedron model can be proposed for  $R\text{O}(3)/\text{O}(4)=3$ , if one assumes that two extra oxygen atoms occupy two O(4) adjacent positions. These two O(4) would share one O(3) which would necessarily form at least one short bond with one of these two O(4). There would be one short bond for every two O(4).

Zolliker et al. [3] reported that a powder pattern

of a  $\text{La}_2\text{CuO}_{4+\delta}$  sample taken by X-ray synchrotron radiation does not show any splitting for the (0 4 1) and (0 6 1) reflections, which are allowed by Cmca but not by Fmmm. Furthermore, these authors were unable to observe by powder neutron diffraction any reflections belonging to the  $\text{La}_2\text{CuO}_{4+\delta}$  phase and violating the F-centering, greater than the experimental detectable intensity limit of about 25% of that of the corresponding reflections belonging to the  $\text{La}_2\text{CuO}_4$  phase.

From our two-phase refinement we calculated the oxygen contribution to each reflection together with the  $I_{hkl}$  intensities for phases 1 and 2. The reflections forbidden by the F-centering are due almost entirely to small contributions from the oxygen atoms which explains why they are not detectable by X-ray diffraction. Furthermore, the contribution to the total intensity of phase 2 for this type of reflections is much smaller than that of phase 1, since these atoms lie closer to the symmetry position required for Fmmm. Often the former is less than 10% of the latter. Among 420 measured reflections violating the F-centering, there are only 9 reflections in which the contribution to the intensity of phase 2 is larger than that of phase 1. This explains why Zolliker et al. could not detect the splitting by neutron diffraction. Some examples of such reflections together with (0 14 0) used in fig. 2 and (1 15 1), both of which are allowed by Fmmm, are illustrated in table V.

Recently Hundley et al. [7] reported the existence of anomalies in the magnetic susceptibility, in the electric resistivity and in the thermoelectric power at about the phase separation temperature. Neverthe-

less, the mechanism leading to the phase separation is not yet understood. By taking into consideration the variation of the reported lattice parameters versus temperature [2,4], below the temperature of the phase separation (about 280 K), the crystal would comprise separate blocks of  $\text{La}_2\text{CuO}_4$  and  $\text{La}_2\text{CuO}_{4+\delta}$ . Zolliker et al. stated that at the phase separation it is the  $\text{La}_2\text{CuO}_4$  phase which is formed. This is in agreement with our observations, and a mechanism can be proposed. Below 280 K, the excess oxygen would diffuse to form oxygen-rich and oxygen-poor blocks. It would be indeed the formation of the  $\text{La}_2\text{CuO}_4$  phase which occurs below 280 K and above this temperature the excess oxygen would be distributed randomly over the entire crystal. The driving force of the oxygen diffusion and consequently of the phase separation would be magnetic in origin. The magnetism of the small oxygen-poor domains existing above 280 K would force the oxygen to diffuse and create oxygen-richer domains. The 0.032 oxygen excess randomly distributed over the entire crystal corresponds to a distribution of the O(4) atoms such that one of every eight  $\text{La}_2\text{CuO}_4$  unit cells would contain an extra oxygen.

### Concluding remarks

The excellent fit of our data using two closely related structure, both in Cmca, suggests a simple phase diagram for the system, similar to that for the PdH system. An immiscibility zone is encountered upon cooling at a critical point, below which the two dis-

Table V  
Structure factor calculation for selected  $hkl$ 's illustrating relative contribution by oxygen scattering.

$h$	$k$	$l$	$F_{\text{oxygen}}^2/F_{\text{total}}^2$	$F_1^2$	$F_2^2$	$F_2^2/F_1^2$	$(F_2^2/F_1^2)_{\text{ext}}^a)$
0	4	1	0.90	7.55	0.75	0.10	
0	6	1	0.52	1.86	0.24	0.13	
2	4	3	0.84	25.23	4.26	0.17	
3	9	6	0.39	26.25	10.65	0.40	
2	4	7	0.68	25.05	15.16	0.60	0.41
0	14	5	0.79	36.38	3.98	0.11	0.14
0	18	3	0.98	49.33	5.34	0.11	0.12
0	14	0	0.02	45.15	67.06	1.49	
1	15	1	0.02	8.90	3.81	2.33	2.22

<sup>a)</sup> Ratios  $(F_2^2/F_1^2)_{\text{ext}}$  are deduced from the data collection on D10. For (0 14 5) and (0 18 3) the doublet peaks are resolved. For (2 4 7) and (1 15 1) the ratio can be obtained by deconvoluting the peaks.



crete phases separate without requiring two different structure types (Fmmm and Cmca). The refined structure of  $\text{La}_2\text{CuO}_{4+\delta}$  with its very weak reflections violating *F*-centering explains the diffraction results previously reported.

The interpretation of the oxygen occupancy factors results in several models, involving either a short bond or normal bonds, and leaves open the question of the exact nature of the defect and how the system is doped. A discrete oxygen at the defect would very likely exist as a charged species and contribute holes to the Cu–O sheets, while a bonded species, very likely as superoxide, would require unexpected electron doping.

#### Acknowledgements

The authors would like to thank Dr. D.E. Cox for making available to them the Zolliker et al. preprint and for the critical reading of this article.

Work at Los Alamos was performed under the aus-

pices of the US Department of Energy, Office of Basic Energy Sciences, Division of Materials Science. Work at Sandia National Laboratories was supported by the US Department of Energy under contract No. DE-AC04-76DP-00789.

#### References

- [1] C. Chaillout, S.W. Cheong, Z. Fisk, M.S. Lehmann, M. Marezio, B. Morosin and J.E. Schirber, *Physica C* 158 (1989) 183.
- [2] J.D. Jorgensen, B. Dabrowski, Shiyu Pei, D.G. Hinks, L. Soderholm, B. Morosin, J.E. Schirber, E.L. Venturini and D.S. Ginley, *Phys. Rev. B* 38 (1988) 11337.
- [3] P. Zolliker, D.E. Cox, J.B. Parise, E.M. McCarron III and W.E. Farneth, preprint.
- [4] J.D. Jorgensen, B. Dabrowski, Shiyu Pei, D.R. Richards and D.G. Hinks, *Phys. Rev. B* 40 (1989) 2189.
- [5] C. Chaillout, J. Chenavas, S.W. Cheong, Z. Fisk, M.S. Lehmann, M. Marezio, B. Morosin and J.E. Schirber, *Physica C* 162–164 (1989) 57.
- [6] P. Wolfers, MXD Refinement Program (unpublished).
- [7] M.F. Hundley, J.D. Thompson, S.W. Cheong, Z. Fisk and J.E. Schirber, *Phys. Rev. B* 41 (1989) 4062.